INTERNATIONAL JOURNAL OF AGRICULTURE & BIOLOGY
ISSN Print: 1560–8530; ISSN Online: 1814–9596
20–1737/2021/26–4–517–526
DOI: 10.17957/IJAB/15.1863
http://www.fspublishers.org

Full Length Article

Biocontrol of Bacteria Associated with Pine Wilt Nematode, *Bursaphelenchus xylophilus* by using Plant mediated Gold Nanoparticles

Joan Shine Davids[1,3], Michael Ackah[1], Emmanuel Okoampah[2,4], Sandra Senyo Fometu[1], Wu Guohua[1*] and Zhang Jianping[1]

[1]*School of Biotechnology, Jiangsu University of Science and Technology, Zhenjiang, P. R. China*
[2]*Department of chemistry and chemical engineering, Biological and environmental discipline laboratory, Jiangsu University of Science and Technology, Zhenjiang, P. R. China*
[3]*Department of biotechnology, Faculty of Biosciences, University for Development studies, Tamale, Ghana*
[4]*Department of biochemistry, Faculty of Biosciences, University for Development studies, Tamale, Ghana*
[*]For correspondence: ghwu@just.edu.cn
Received 15 December 2020; Accepted 14 July 2021; Published 28 September 2021

Abstract

Following the discovery of *Bursaphelenchus xylophilus* as the causative organism of pine wilt disease (PWD), the development of an effective and efficient pesticide to control the spread of PWDs is necessary to avoid economic and environmental losses. Over time, patents and products that use nanomaterials in agricultural practices, such as nano-fertilizers, nano-pesticides and nano-sensors, among others, have emerged to ensure efficient and sustainable agriculture. In this paper, *Parkia biglobosa* leaf (PL-AuNPs) and stem (PS-AuNPs) mediated gold nanoparticles were used as antimicrobials against some isolated symbiotic bacteria (*Pseudomonas syringae, Escherichia coli, Staphylococcus aureus and Bacillus anthracis*) from pine wood nematode. Preliminary qualitative phytochemical studies confirmed the presence of cardiac glycosides, flavonoids, saponins, proteins and steroids in both the leaves and stem except for terpenoids and alkaloids which was present in the stem only. The as-synthesized AuNPs were characterized by UV-Vis spectrophotometer, Transmission electron microscope, X-ray diffraction, and Fourier-transmission infrared. The UV-vis recorded plasmon resonance of 530 nm for both PS-AuNPs and PL-AuNPs. The TEM of the leaf nanoparticle exhibited mono-dispersed particles with the shape to be spherical, triangular and irregular, and rod-shaped with sizes ranging from 2.5 nm to 25 nm whiles the TEM of the PS-AuNPs revealed truncated, pentagonal, nanorod, spherical, triangular shape with sizes 1 to 35 nm. However, the FTIR also exhibited the presence of O-H group (phenols) in the AuNPs and the XRD showed the AuNPs are crystalline with cubic structure. The various AuNPs exhibited high antimicrobial activity against the symbiotic bacteria by inhibiting their growth. PS-AuNPs and PL-AuNPs recorded an inhibition zone of 50.50 and 51 mm ,46 mm and 37.5 mm, 62 and 66 mm, 42.5 and 40 mm against *Pseudomonas syringae, Escherichia coli, Staphylococcus aureus* and *Bacillus anthracis,* respectively. The gold salt (G.S) used as a control showed no inhibition against the bacteria. This had shown the potential of biosynthesized AuNPs to shorten the lifespan of the *B. xylophilus* associated symbiotic bacteria by inhibiting their growth, thereby preventing further damage to pinewood demonstrating the ethnobotanical relevance of AuNPs incorporation in pesticide development to combat pathogenic parasites and elucidating the bio-reductive and stabilizing activity of chloroauric gold ($HAuCl_4$) using plants and plant parts.

Keywords: Biosynthesis; Gold nanoparticles; *Parkia biglobosa*; Pine wood nematode; Pine Wilt disease

Introduction

Plant-infectious diseases caused by pinewood nematodes (PWN) have become alarming over the years and causing significant damage to pinewood despite efforts to contain them. Ethnobotanical studies have revealed the causative agent of pine wilt disease to be *B. xylophilus*. Preliminary investigation reported *B. xylophilus* to be native to North-America and later introduced to Japan and subsequently spread into China, Korea and into Europe (Portugal and Spain) (Proença *et al*. 2010). Prior to the inception of PWNs, research studies have revealed the association of possible toxin producing bacteria. These bacteria enter a symbiotic relationship with the PWN as a way of extending their lifespan in the pinewood. The activity of the so-called symbiotic bacteria within the pinewood lead to plant damage by destroying the absorption and transportation systems of plants which subsequently leads to wilting and eventual death (Alves *et al.* 2018; Su *et al.* 2020). PWNs convey varying bacterial diversity depending on the country

and location (Vicente *et al.* 2011). Nonetheless, it has been hypothesized that differences in bacterial community structure in different forest ecosystems are the cause of differences in bacterial species associated with the pine wood nematode (PWN) in certain areas which tend to justify the pathophysiology of pine wilt diseases (PWD). With PWD native to America, *Cedrus deodara*, for example, has been reported to be predominant in the United States (Wingfield *et al.* 1982) and Japan (Mamiya 1983), while *Pseudomonas* seems to be the abundant in China (Proença *et al.* 2010; Zhao *et al.* 2011).

The Potency of already existing control measures for associated symbiotic bacteria of PWDs remains unspecified as reports indicate that these measures tend not to have the full potential to control PWNs and in some cases causes environmental perturbation (Sabry 2019). For instance, the major treatment explored for treating PWDs which involve the spraying of insecticides has been reported to be inadequate to discontinue the spread of the damages of the symbiotic bacteria (Shinya *et al.* 2013). The issue therefore makes it obligatory to seek new antimicrobials and/or new effective means of treating infectious diseases triggered by bacteria associated with pine wilt disease (PWD).

The surging advancement of nanotechnology in agriculture has gained substantial consideration worldwide since it can be applied to any system of agriculture through potential and well-ordered release and targeted supply of agrochemicals towards PWN (Jo *et al.* 2009; Servin *et al.* 2015; Sabry 2019). For instance, developing a pesticide incorporated with AuNPs have been reported to be lethal to nematodes without any negative impact on plants (Tsyusko *et al.* 2012; Thakur and Shirkot 2017). This has spurred interest in studying the antibacterial action of NPs against PWNs (Vallet-Regí *et al.* 2019). Several research investigations have been focused on the drug delivery and disease site targeting efficiency of NPs since their introduction, which is relevant to their usage as a control option to nematode infections. Nonetheless, the efficacy and activities of NPs in agriculture lies with their synthesis approach. Over the period, researchers has extensively explored the conventional chemical synthesis approach of obtaining NPs (Xu *et al.* 2007; Luty-Błocho *et al.* 2011; Ojea-Jiménez *et al.* 2011; Ansari *et al.* 2020), however, the chemical synthesis approach has been reported to be toxic especially in an *in vivo* experiment (Goodman *et al.* 2004; Chen *et al.* 2009; Lasagna-Reeves *et al.* 2010). It is therefore necessary to resort to a safer and simpler approach of NPs synthesis that involves using plants and their parts. In our recent work, we successfully synthesized a novel AuNPs using only leaf extract of *Parkia biglobosa* and investigated its potential to inhibit the growth of some selected clinical isolates (Shine *et al.* 2020). Also, Akintelu *et al.* (2021) used *Garcinia kola* pulp extract to synthesize gold nanoparticles and explored it antibacterial potency. It is against this background, *Parkia biglobosa*, a popular medicinal plant in the northern Ghana is used both as reducing and stabilizing agents to obtain gold nanoparticles from the reduction of chloroauric gold ($HAuCl_4$) from Au^{3+} to Au^0. The as-synthesized AuNPs were explored for their antimicrobial potential against isolated symbiotic bacteria (*Staphylococcus Aureus, Pseudomonas Syringae, Bacillus Anthracis* and *Escherichia Coli*) from pine wilt nematode, *B. xylophilus*. The biosynthesized AuNPs has the potential to shorten the lifespan of the *B. xylophilus* associated symbiotic bacteria by inhibiting their growth to curtail a further damage to pinewood.

Materials and Methods

$HAuCl_4$ was obtained from Sigma Aldrich, Pine branches were collected from the suburbs of Zhenjiang (Jiangsu, China). *Parkia biglobosa* leaf and stem bark were also obtained from the university for development studies, Tamale, Ghana.

Source, isolation, and culture of nematode (*Bursaphelenchus xylophilus*)

The isolation of the nematodes used in this experiment followed the protocol by (Han *et al.* 2003; Zhang *et al.* 2014). Naturally, infected (symptomatic) black pine (*Pinus thunbergii*) tissues were cut into small chips of about 1×1 cm pieces using a saw and cutter. The chips were weighed with an electronic balance. Total chips of 162 g were divided into groups of units with each at 20 g. Using the Baermann funnel method as described by (Zhang *et al.* 2014), with some modification, about 20 g of the chips were put on a cheesecloth placed inside the Baermann funnel. Warm water at about 25°C was used to soak the chips in the funnel and ice water bottles were put beneath the end of the funnel tube to maintain ample cold temperatures. The setup was put into an incubator and left for 6 h. Nematode suspension was collected after 6 h. 2 mL of the solution was taken to observe the presence and population of nematode under a high-power microscope (Caikon XTL, China). The nematode was identified as *B. xylophilus* cultured with the fungus *Botrytis cinerea* on a low nitrogen potato dextrose agar (PDA) plate. Subsequently, the plates were further incubated until the fungal mycelia were entirely consumed by the nematodes and then separated from the culture medium by using a Baermann funnel to obtain an aqueous suspension of nematodes for a subsequent test.

Isolation and culture of bacteria strains from nematodes body

In this study, Strains of bacteria were isolated from the body of *B. Xylophilus* by raw liquid and washed liquid treatments. In the raw liquid treatment, nematode suspension containing about 1200 nematode population was ground (with a push and pull, up to 40 oscillations using a mortar and pestle) under aseptic conditions. The suspension was diluted to

different gradients (10^{-3}, 10^{-4}, 10^{-5}) and cultured on a Petri dish containing beef extract medium (NA) at a concentration of (0.005 g/mL, 1.99 g/mL and 8.0 g/mL), with (4) plates as technical replicates. The same procedure was repeated for PDA medium at a concentration of (0.02 g/mL, 0.2 g/mL, 0.07 g/mL and 0.04 g/mL). The coated plates were incubated at 20–24°C to observe bacteria growth.

In the washing liquid treatment procedure, a nematode solution containing about 2000 nematode population was taken and shook vigorously in low-temperature cold water for 200 times and then centrifuged at 8000 rpm after which the supernatant was removed and washed with sterile water 2–3 times. The mixture was grounded under aseptic conditions and then diluted to various concentrations (10^{-2}, 10^{-3} and 10^{-4}). These were coated on the beef extract and PDA medium as described above and incubated at 20–24°C to observe bacteria growth. Bacteria growth was observed 4–5 days after inoculation (DAI). Several bacterial colonies were marked from the various plate containing different treatments. Using bacterial characteristics such as morphology, shape, color, colonies of the bacteria strains were isolated into the freshly prepared medium. Pure bacteria colonies were isolated with beef extract medium in a slanted and liquid tube and preserved for subsequent use.

Gram staining and Molecular Identification isolates

The microscope was used to identify isolated bacteria. Gram stain was done to classify the bacteria into gram-positive and gram-negative. Bacteria single colonies representing each bacteria obtained from the culture plates were further identified by molecular method following the protocol (Kai *et al.* 2019) by using 16S rRNA gene sequence. The samples were sequenced by Nanjing Huizhi Zhiyuan Biotechnology Co., Ltd., China.

Extraction and Phytochemical screening

The samples were defatted and 8 g each of the leaves and stem powder was measured into 25 mL beaker each. 24 mL of hexane was added to the samples. The solution was stirred continuously for 90 min by use of a magnetic stirrer. The stirring was stopped and the sample left for 30 min before decanting. The sample was then filtered under vacuum and subjected to extraction and phytochemical screening. The screening techniques were carried as reported by (Akinyemi *et al.* 2005).

Test for flavonoids

1 mL of aqueous extract was added to 1 mL of 10% lead acetate solution. The formation of a yellow precipitate was taken as a positive test for flavonoids.

Test for Alkaloids

3 mL of aqueous extract was stirred with 3 mL of 1% HCl on a steam bath. Mayer's and Wagner's reagents were then added to the mixture. Turbidity of the resulting precipitate was taken as evidence for the presence of alkaloids.

Test for tannins

About 2 mL of the aqueous extract was stirred with 2 mL of distilled water and few drops of $FeCl_3$ solution added. The formation of a green precipitate was an indication for the presence of tannins.

Test for saponins

5 mL of aqueous extract was shaken vigorously with 5 mL of distilled water in a test tube and warmed to 100°C. The formation of stable foam was taken as an indication for the presence of saponins.

Test for terpenoids

2 mL of the organic extract was dissolved in 2 mL of chloroform and evaporated to dryness. 2 mL of concentrated sulphuric acid was then added and heated for about 2 min. A greyish colour indicates the presence of terpenoids.

Tests for steroids

2 mL of ethanol extract was dissolved in 2 mL of chloroform and 2 mL concentrated sulphuric acid were added. Formation of a red colour in the lower chloroform layer was used as an indicator for the presence of steroids.

Tests for carbohydrates

To 3 mL of the aqueous extract was added about 1 mL of iodine solution. A purple colouration at the interphase indicates the presence of carbohydrate.

Tests for glycosides

Salkowski's test

2 mL of each extract was dissolved in 2 mL of chloroform. 2 mL of sulphuric acid was added carefully and shaken gently. A reddish brown colour indicates the presence of a steroidal ring (that is a glycone portion of glycoside).

Tests for anthraquinones

Borntrager's test

3 mL of aqueous extract was shaken with 3 mL of benzene, filtered and 5 mL of 10% ammonia solution was added to the filtrate. The mixture was shaken and the presence of a pink, red or violet colour in the ammoniacal (lower) phase indicates the presence of free anthraquinones.

Test for proteins

Buiret's test

A 2 mL of aqueous extract was added to the buiret's reagent. The color changed to purple showing presence of protein.

Biosynthesis

Measure 5 g of powdered leaf and stem into two different beakers and add 25 mL of deionized water to each sample. Stir to obtain a homogenous mixture and was left for 24 h. The samples were filtered using Whatman filter paper. 9 mL of 1MHauCl_4 was measured into two beakers and 1 mL each of the leaf and stem was added to the HauCl_4. A pronounced colour change was observed for both leaf and stem where the leaf mediated AuNPs exhibited a dark purple colour while that of the stem was ruby red.

Characterization

After colour change was observed Ultraviolet-visible spectrophotometer (SpectraMax i3, Silicon Valley USA) was used to determine the plasmon resonance. A 96 well costar clear plate was used for the analysis of the AuNPs, and water was used as the blank. Transmission Electron microscopy (TEM) was used to analyze the shape, sizes, and dispersion of the gold transmission electron microscope (TEM). It was performed TEM was performed on a field emission transmission electron microscope (Tenai G2 F30 S-TWIN, FEI) at an acceleration voltage of 300 kV. FT-IR was also used to analyze the functional group of the NPs. Further analysis was done by XRD to ascertain the crystallinity of the gold nanoparticles. The purified purified freeze-dried AuNPs were blended with KBr to obtain pellet and were subjected to FTIR spectroscopy. The FT-IR spectra were measured at a resolution of 4 cm^{-1} in the transmission mode (4000 cm^{-1}–400 cm^{-1}) Fourier transform infrared spectroscopy (FTIR) on a Bruker spectrometer (Tensor 27).

Antibacterial study

0.9 g of nutrient broth was measured into a 100 mL beaker and 50 mL of water added. The culture media was then measured 2 mL each into a glass tube and autoclaved for 15 min at 121ºC. The media was afterward inoculated with the isolated bacteria for re-culturing. The inoculum was then incubated for 18hrs and shook at 230 ppm. 9.5 g of Mueller Hinton agar was measured into 250 mL of water, stirred, and autoclaved at 15 min with punched paper disks and the Petri dishes. After sterilizing, the agar was distributed to the Petri dishes and allowed to solidify. Whiles awaiting the solidification of the agar, the paper discs of diameter 6 mm were impregnated with 5 *u*L/mL of the gold nanoparticles. A cotton swab was used to smear the culture on the agar and incubated for 24 h at 37ºC. The inhibition zone was evaluated using a straight rule.

Statistical analysis

The data was analysed using Genstat 11th edition in a One-way analysis of variance (ANOVA) and the results presented as mean of three replicates. Means separation was done using bonferroni tests at 5% significant level.

Results

The microscope was used to identify isolated bacteria. Gram stain was done to classify the bacteria into gram-positive and gram-negative. The pink colour indicating gram-negative while purple represents gram-positive bacteria and their morphology were used to specify them. *Staphylococcus aureus* is as represented in Fig. 3A and 3B is a Gram-positive round-shaped bacteria that is a member of the Firmicutes, usually part of the microbiota of the body in the forms of germs found on the skin or in even a healthy individual's nose causing skin, bone, joint and respiratory infections (Curran and Al-Salihi 1980; Cole *et al.* 2001).

Pseudomonas syringae on the other hand is a rod-shaped, Gram-negative bacterium with polar flagella as exhibited in Fig. 3C and 3D. It is a host-specific pathogen whose interactions in plants can take two strikingly courses. Thus, in virulent interactions with susceptible plants, the bacteria multiply for several days before producing visible symptoms such as necrotic lesions on leaves and fruits whiles the avirulent interactions with resistant plants the bacteria trigger a rapid localized, defense-associated, programmed death cell known as the hypersensitive response (Collmer *et al.* 2002).

Bacillus anthracis is *a* Gram-positive, endospore-forming rod-shaped bacterium with a width of 1.0–1.2 and µm and a length of 3–5 *µ*m as shown in Fig. 3E and 3F. Bacillus anthracis is the anthrax agent, a prevalent animal and sometimes human disease and the only mandatory pathogen in the genus *Bacillus* (Spencer 2003). This disease can be known as a zoonosis, because by transmitted from infected animals to humans has long been considered a potential biological weapon (Spencer 2007).

E. coli as shown in Fig. 3G and 3H is a Gram-negative, facultatively anaerobic, rod-shaped, coliform bacterium of genus *Escherichia* that is commonly found in the lower intestine of warm-blooded organisms (Singleton 2004; Tenaillon *et al.* 2010). After the gram staining to obtain the morphotype of the strains, molecular identification was carried out using 16RS sequencing (Supporting information).

The present study focused mainly on the qualitative chemical evaluation of the phytochemical constituents of extract from the stem and leaves of *Parkia biglobosa*. The study revealed the presence of alkaloids, tannins, cardiac glycosides and flavonoids, terpenoids, saponins and

glycosides in the stem whiles the leaves exhibited cardiac glycosides, flavonoids, saponins, alkaloids, proteins, and amino acids and steroids (Table 1). The phytochemicals present have been shown to possess medicinal activity as well as physiological activity in previous studies by (Udobi and Onaolapo 2009; Builders *et al.* 2012). These results show that *Parkia biglobosa* stem and leaves can be a potential source of useful compounds that can be used to synthesize nanoparticles for new antimicrobial drugs. The presence of these phytochemicals justifies the traditional medicinal uses of this plant by the local people in West and East Africa.

The initial colour of the plant extracts was brown whiles the gold salt was yellow however after adding the plant extracts to the gold salt, a colour change was optically observed. The colour of the leaf mediated-AuNPs was dark purple while that of the stem mediated-AuNPs was observed to be ruby red. Thereafter, the UV-vis was used to determine the plasmon resonance and the absorbance with the range of wavelength 230–1000 nm with 5 min intervals for 30 min. It was revealed in Fig. 1 and 2A and B that the plasmon resonance was recorded at 530 nm for both the L-AuNPs and S-AuNPs. The absorbance for L-AuNPs started from 2 min whiles that of stem started from 3 min and progressively rise as the time increases till it attained stability.

The leaf mediated AuNPs also had an optical colour change from dark brown to dark purple and were supported with the UV-vis registering absorbance from 2 min and completed at around 30 min.

The TEM exhibited the shape of the Leaf nanoparticle to be spherical, triangular, and irregular, and rod-shaped as demonstrated in Fig. 3A, B and C.

Conversely, the complete synthesis of the stem mediated AuNPs was observed at 30 min as indicated in Fig. 2B accompanied by a colour change from dark brown to ruby red. As shown in Fig. 3D, E and F, the TEM revealed truncated, pentagonal, nanorod, spherical, triangular shape with sizes 3–28 nm.

From Fig. 4A, the FT-IR of the leaf revealed bands at 615 Cm^{-1}, 777 Cm^{-1} 1060 Cm^{-1} 1143 Cm^{-1} 1394 Cm^{-1} 1630 Cm^{-1} 2038 Cm^{-1}, 2860 Cm^{-1} 2937 Cm^{-1}, 3303 Cm^{-1} 3487 Cm^{-1}. The band revealed at 615 Cm^{-1} and 3303 Cm^{-1} could be a C-H stretch vibrations while that of 777 Cm^{-1} can be attributed to aromatic C-H bend, 1143 Cm^{-1} C-O stretch, 1394 CH3 C-H. An intense band located at 1630 Cm^{-1} was attributed to benzene ring stretch however the band at 2038 Cm^{-1} was not assigned. The band at 2860 Cm^{-1} and 2937 Cm^{-1} correspond to aliphatic CH stretch 3487 Cm^{-1} can also be likened to O-H stretching and N-H stretching vibrations, respectively.

On the other hand, as exhibited in Fig. 4B, the stem also revealed bands at 613 Cm^{-1} C-H stretch vibrations, 793 Cm^{-1} aromatic CH vibrations which could be alkanes. 1080 Cm^{-1} C-C stretching vibrations, 1279 Cm^{-1} C-O stretching vibrations, 1614 Cm^{-1} Aromatic C=C stretching, 2085 Cm^{-1} C=conjugated 2922 Cm^{-1} asymmetrical stretching CH_2, 3311 Cm^{-1} and 3465 Cm^{-1} could be assigned OH stretch (alcohols Phenols). From the FT-IR results of the S-AuNPs, we hypothesized phenolic compounds and flavonoids to be responsible for the reduction process and stabilization of the AuNPs. This finding is supported by experiments carried out by (Gopinath *et al.* 2014; Markus *et al.* 2017; Chahardoli *et al.* 2018).

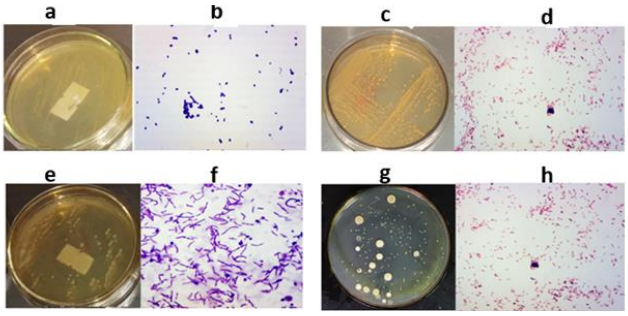

Fig. 1 a) A plate showing *Staphylococcus aureus* colonies of agar **b**) A plate exhibiting gram-stain of *Staphylococcus aureus*, **c**) A plate showing *Pseudomonas syringae* colonies on agar **d**) A plate showing gram stain of *Pseudomonas syringae*, **e**) A plate showing *Bacillus anthracis* colonies on agar, **f**) A plate showing gram stain *Bacillus anthracis*

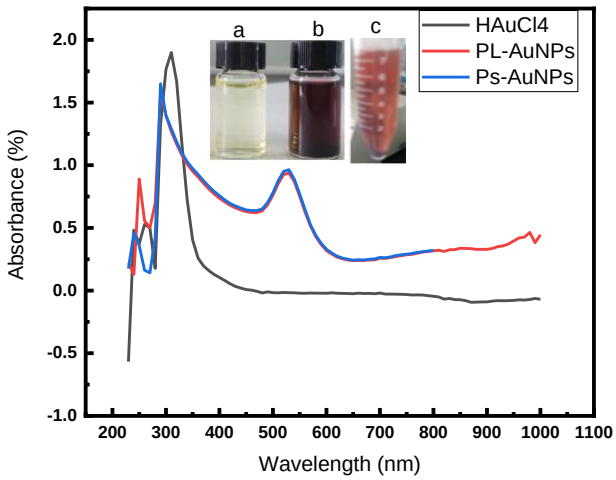

Fig. 2: Uv-vis absorption spectrum of **a**) Chloroauric gold, **b**) leaf-mediated gold nanoparticle, **c**) stem-mediated gold nanoparticles

Table 1: Phytochemical analysis of ethanolic leaf and stem extract

Phytochemical Test	Stem	Leaves
Cardiac glycosides	+	+
Flavonoids	+	+
Terpenoids	+	-
Anthraquinones	-	-
Saponins	+	+
Glycosides	+	+
Alkaloids	+	+
Carbohydrates	-	-
Tannins	+	-
Proteins and amino acids	-	+
Steroids	-	+

Inference (+) = Present (-) = Absent

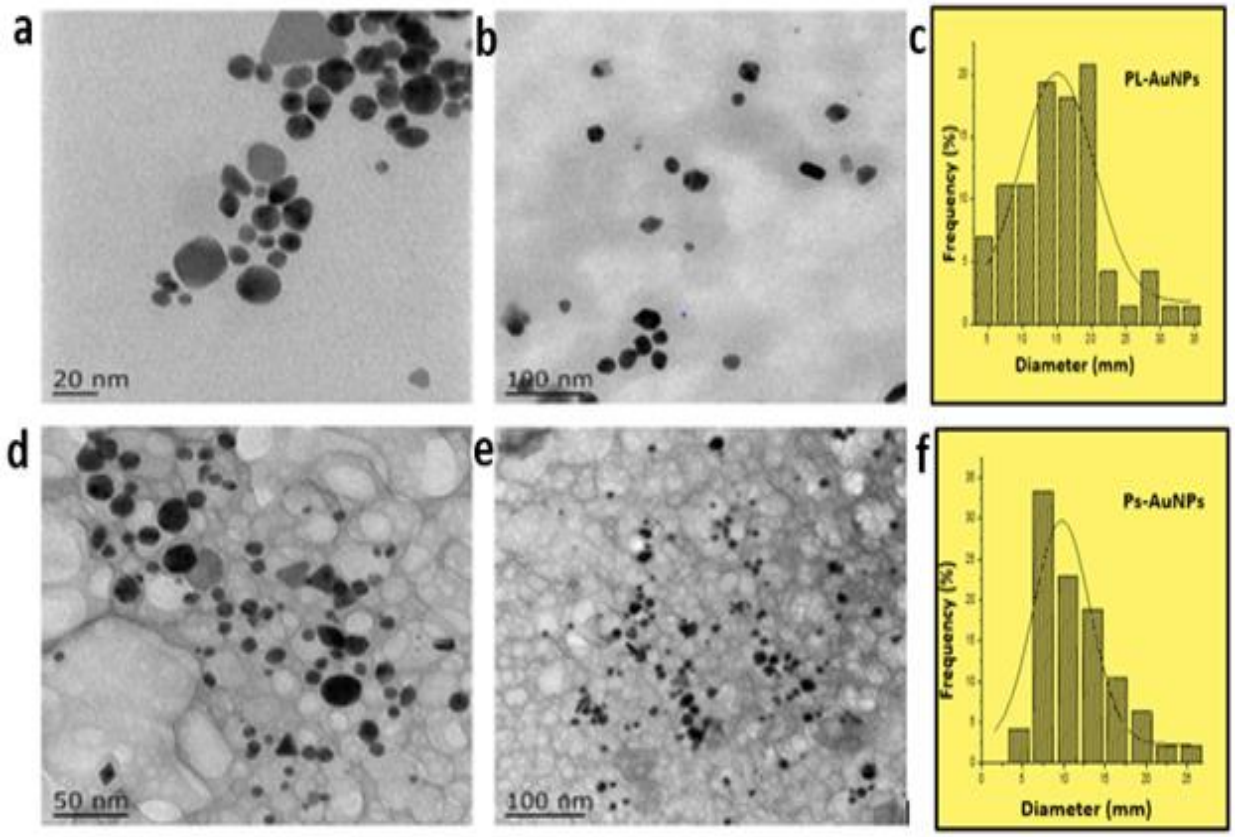

Fig. 3: a) Transmission electron micrograph of the Leaf- meditated AuNPs on a scale of 20 nm, **b**) Transmission electron micrograph of the Leaf- meditated AuNPs on a scale of and 100 nm, **c**) Transmission electron distribution graph of Leaf- meditated AuNPs, **d**) Transmission electron micrograph of the stem mediated AuNPs 20 nm, **e**) Transmission electron micrograph of the stem mediated AuNPs on the scale of 100 nm, **f**) Transmission electron distribution graph stem mediated AuNPs

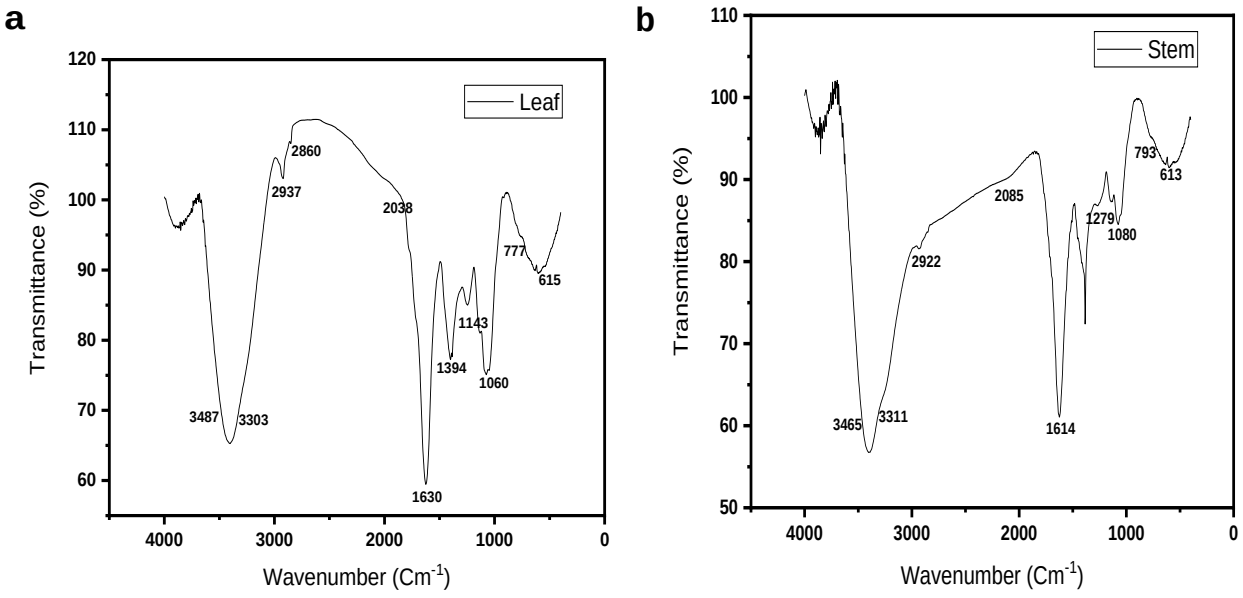

Fig. 4 a) Fourier Transmission Infrared of the leaf mediated nanoparticles, **b**) Fourier Transmission Infrared of the stem mediated nanoparticles

Table 2: Antibacterial screening of *Parkia biglobosa* stem and leaf mediated AuNPs against the bacteria isolates (Data were expressed as mean of 3 replicates)

Bacteria strain	Inhibition Zone (mm)		
	G-S	L-AuNPs	S-AuNPs
B. A	0.00	40.00	42.50
E.C	0.00	37.50	46.00
P. S	0.00	51.00	50.50
S. A	0.00	62.50	66.00

Inference B.A=*Bacillus anthracis* E.C. *Escherichia coli*, P.S *Pseudomonas syringae*, S.A *Staphylococcus aureus*

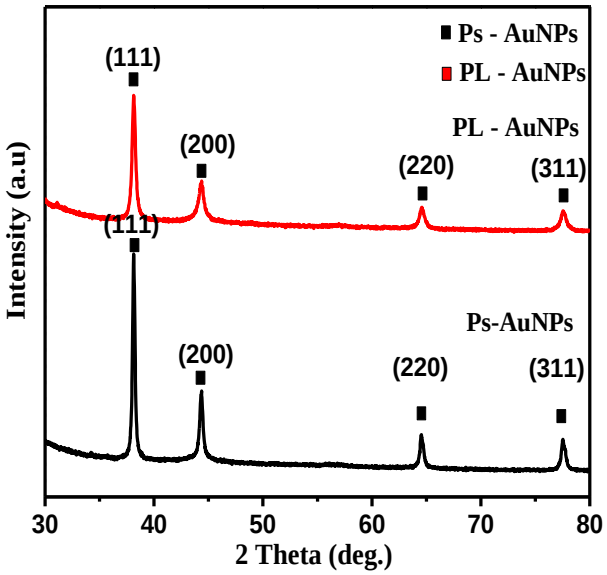

Fig. 5: X-ray powder diffraction graph of the stem- AuNPs and

The FT-IR results show the presence of phenols which could be the reduction agent for the AuNPs (Sadeghi *et al.* 2015; Markus *et al.* 2017; Chahardoli *et al.* 2018).

To further probe into the crystal structure of the AuNPs synthesized, X-ray diffraction (XRD) experiment was performed which revealed that, both PS-AuNPs and PL-AuNPs displayed four pronounced diffraction peaks corresponding to the (111), (200), (220) and (311) planes of Au, at a 2θ of approximately 38.184°, 44.392°, 64.578° and 77.547°, respectively as shown in Fig. 5 and 6 above. In totality, the planes and peaks observed with the gold nanoparticles are, respectively, the typical peaks for the (111), (200), (220) and (311) planes of Au (JCPDS: 04–0784) NPs, indicating the successful synthesis of a reduction of the chloroauric gold to obtain gold nanoparticles with a cubic structure, Fm-3m (225). The intensity of the (111) peak is much stronger than those of other peaks, suggesting that the Au (111) plane is the predominant crystal facet in the synthesized Au nanoparticles.

As represented in Table 2 above the AuNPs tested against the *Pseudomonas syringae* recorded an inhibition of 50.50 mm for the PS-AuNPs and 51 mm for the PL-AuNPs. Moreover, the zone of inhibition of *Escherichia coli* was evidenced for PS-AuNPs at 46 mm whiles that of PL-AuNPs was recorded at 37.5 mm. Notwithstanding a significant inhibition of PS-AuNPs at 62 mm and PL-AuNPs had an inhibition zone at 66 mm for *Staphylococcus aureus*. The gold nanoparticles colloids also had an inhibition on the growth of *Bacillus anthracis* where PS-AuNPs inhibited to a diameter of 42.5 mm whiles PL-AuNPs recorded 40 mm. Lastly, the G.S however did not have any inhibition on the isolates.

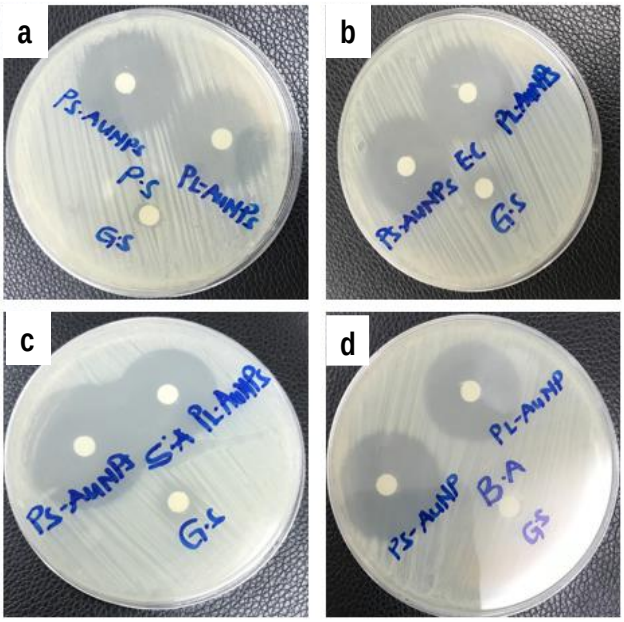

Fig. 6: Plates with the zone of inhibition of both the stem-mediated AuNPs (PS-AuNPs) and Leaf-mediated AuNPs (PL-AuNPs) against; **a**) *Pseudomonas syringae* (P.S), **b**) *Escherichia coli*. (E.C), **c**) *Staphylococcus aureus* (S.A), **d**) *Bacillus anthracis*

Discussion

Pseudomonas syringae, *Escherichia coli*, *Staphylococcus aureus* and *Bacillus anthracis* were identified. *Pseudomonas syringae* is a gram-negative bacteria pathogen that infects over 50 species of pathovars leading to canker and leaf spots in plants. *Escherichia coli* is a causative agent of gastrointestinal infections (Cabral 2010), normally found in contaminated water and food. *Bacillus anthracis* on the other hand is a gram-positive bacterium classified as zoonotic because it infects both humans and animals. It causes anthrax which may be fatal in some cases. Similarly, *Staphylococcus aureus* is a gram-positive bacterium associated with skin and respiratory infections.

The disk diffusion method was used to evaluate the antibacterial efficacy of the bacteria isolates. Our findings recorded for both stem and leaf mediated synthesized AuNPs at 50% each for *Pseudomonas syringae* supports works done by (Mishra *et al.* 2014). Moreover, our

susceptibility reports of the AuNPs on the inhibition of *E. coli* are supported by (Ali *et al.* 2011). The results of the biosynthesized gold nanoparticle inhibiting the growth of the *Bacillus anthracis* are, however, in contrast to a report by (Abbai *et al.* 2016) who stated that AuNPs did not have any inhibition efficacy on *Bacillus anthracis* in their study conducted.

It was realized that the effectiveness of the AuNPs on the gram-positive bacteria compared to gram-negative bacteria is significant. This is because the cell wall of gram-positive bacteria is single-layered which allows easy entry of the nanoparticles, whiles the cell wall of the gram-negative bacteria is wavy and double-layered. Although the mechanism of AuNPs activities in the inhibition of the growth bacteria is not well documented, gold nanoparticles has been reported to create holes in the cell wall, allowing cell contents to leak, resulting in cell death (Mishra *et al.* 2014). The potency of metal nanoparticles against bacterial pathogens can also be due to the presence of antibacterial macromolecules, such as proteins and enzymes which are adsorbed on the surface of synthesized nanoparticles and which increase the antimicrobial activity of nanoparticles (Balakumaran *et al.* 2016). As a potential mechanism, AuNPs can bind to the important characteristics of the bacterial outer membrane and thus lead to structural changes, degradation and ultimately cell death. This is because they interact with the DNA in the bacterial cells and interfere with the transcription of the strain's DNA, resulting in stunted growth and cell damage (Bauer *et al.* 2004; Rai *et al.* 2010; Srivastava and Mukhopadhyay 2015). The present results in the treatment of *E. coli* and *S. aureus* with biosynthesized AuNPs showed a higher inhibition as compared to the reports of researchers using various plant extracts such as *Prunus armeniaca*, *Curcuma pseudomontana*, *Carica papaya*, *Solanum nigrum*, *Areca catechu* (Muniyappan and Nagarajan 2014; Muthuvel *et al.* 2014; Rajan *et al.* 2015; Srivastava and Mukhopadhyay 2015; Muthukumar *et al.* 2016). This could be due to the different bacteria strains, the different structure and composition of cell walls and the smaller sizes of the *P. biglobosa* mediated AuNPs produced. Factors such as the phytochemical composition of the plant extracts, properties of the nanoparticles, and particle shape and surface can also be involved in the site-specific reaction of bacterial strains. The ineffectiveness of the G.S on the isolates could be attributed to the large particle size of the gold salt which did not allow penetration through the cell wall of the bacterial strains.

Conclusion

A biosynthesized nanoparticle was obtained by using the leaf and stem extracts of *Parkia biglobosa* to reduce chloroauric gold to obtain their nanoparticles form. The *Parkia biglobosa* mediated AuNPs were evaluated by UV-Vis, FTIR, TEM, and XRD which confirmed the successful synthesis of AuNPs. The as-synthesized AuNPs were able to inhibit the growth of the symbiotic bacteria isolated from the Pine Wilt Nematode with the highest inhibitory activity from the greatest to the lowest in the order *staphylococcus aureus* < *Pseudomonas syringae* < *Bacillus anthracis* < *Escherichia coli.* This method of producing NPs by employing plants and plant components has proven to be a viable option for obtaining toxic-free NPs safe for biomedical and pharmaceutical application. With the extensive research into NPs for antimicrobial properties, their use in pesticide production will demonstrate a new generation way of an improved agricultural practices.

Acknowledgement

The authors immensely acknowledge the financial supports from Jiangsu special Approved Professor Program Sujiaoshi ([2015]17).

Author Contributions

Joan Shine Davids: Conceptualization, Data curation, Formal analysis, Investigation, Methodology, Writing original draft; Micheal Ackah: Resources, visualization; Emmanuel Okoampah: Writing review and editing; Sandra Senyo Fometu: Writing review and editing; Zhang Jianping: Supervision, analysis; Wu Guohua: Funding Acquisition, Project administration, supervision, Validation.

Conflict of Intrest

Authors declare no conflicts of interests among institutions.

Data Availability

This work does not involve animals hence.

Ethics Approval

Not applicable to this article.

References

Abbai R, R Mathiyalagan, J Markus, YJ Kim, C Wang, P Singh, S Ahn, ME-A Farh, DC Yang (2016). Green synthesis of multifunctional silver and gold nanoparticles from the oriental herbal adaptogen: Siberian ginseng. *Intl J Nanomed* 11:3131–3143

Akintelu SA, B Yao, AS Folorunso (2021). Green synthesis, characterization, and antibacterial investigation of synthesized gold nanoparticles (AuNPs) from *Garcinia kola* pulp extract. *Plasmonics* 16:157–165

Akinyemi KO, O Oladapo, CE Okwara, CC Ibe, KA Fasure (2005). Screening of crude extracts of six medicinal plants used in South-West Nigerian unorthodox medicine for anti-methicillin resistant *Staphylococcus aureus* activity. *BMC Compl Altern Med* 5; Article 6

Ali DM, N Thajuddin, K Jeganathan, M Gunasekaran (2011). Plant extract mediated synthesis of silver and gold nanoparticles and its antibacterial activity against clinically isolated pathogens. *Colloids Surf B* 85:360–365

Alves M, A Pereira, C Vicente, P Matos, J Henriques, H Lopes, F Nascimento, M Mota, A Correia, I Henriques (2018). The role of bacteria in pine wilt disease: insights from microbiome analysis. *FEMS Microbiol Ecol* 94:1–13

Ansari RA, R Rizvi, I Mahmood (2020). *Management of Phytonematodes: Recent Advances and Future Challenges*, 1st edn, Springer, Singapore

Balakumaran M, R Ramachandran, P Balashanmugam, D Mukeshkumar, P Kalaichelvan (2016). Mycosynthesis of silver and gold nanoparticles: Optimization, characterization and antimicrobial activity against human pathogens. *Microbiol Res* 182:8–20

Bauer LA, NS Birenbaum, GJ Meyer (2004). Biological applications of high aspect ratio nanoparticles. *J Mater Chem* 14:517–526

Builders M, C Isichie, J Aguiyi (2012). Green synthesis of gold nanoparticles from fruit extract of *Terminalia arjuna*, for the enhanced seed germination activity of *Gloriosa superba*. *J Nanostruct Chem* 4; Article 115

Cabral JP (2010). Water microbiology. Bacterial pathogens and water. *Intl J Environ Res Publ Health* 7:3657–3703

Chahardoli A, N Karimi, F Sadeghi, A Fattahi (2018). Green approach for synthesis of gold nanoparticles from *Nigella arvensis* leaf extract and evaluation of their antibacterial, antioxidant, cytotoxicity and catalytic activities. *Artific Cells Nanomed Biotechnol* 46:579–588

Chen YS, YC Hung, I Liau, GS Huang (2009). Assessment of the *in vivo* toxicity of gold nanoparticles. *Nanoscale Res Lett* 4:858–864

Cole AM, S Tahk, A Oren, D Yoshioka, YH Kim, A Park, T Ganz (2001). Determinants of *Staphylococcus aureus* nasal carriage. *Clin Diagn Lab Immunol* 8:1064–1069

Collmer A, M Lindeberg, T Petnicki-Ocwieja, DJ Schneider, JR Alfano (2002). Genomic mining type III secretion system effectors in *Pseudomonas syringae* yields new picks for all TTSS prospectors. *Trends Microbiol* 10:462–469

Curran JP, FL Al-Salihi (1980). Neonatal staphylococcal scalded skin syndrome: Massive outbreak due to an unusual phage type. *Pediatrics* 66:285–290

Goodman CM, CD McCusker, T Yilmaz, VM Rotello (2004). Toxicity of gold nanoparticles functionalized with cationic and anionic side chains. *Bioconjug Chem* 15:897–900

Gopinath K, S Gowri, V Karthika, A Arumugam (2014). Green synthesis of gold nanoparticles from fruit extract of *Terminalia arjuna*, for the enhanced seed germination activity of *Gloriosa superba*. *J Nanostruct Chem* 4:115

Han Z, Y Hong, B Zhao (2003). A study on pathogenicity of bacteria carried by pine wood nematodes. *J Phytopathol* 151:683–689

Jo YK, BH Kim, G Jung (2009). Antifungal activity of silver ions and nanoparticles on phytopathogenic fungi. *Plant Dis* 93:1037–1043

Kai S, Matsuo, S Nakagawa, K Kryukov, S Matsukawa, H Tanaka, T Iwai, T Imanishi, K Hirota (2019). Rapid bacterial identification by direct PCR amplification of 16S rRNA genes using the MinION™ nanopore sequencer. *FEBS Open Bio* 9:548–557

Lasagna-Reeves C, D Gonzalez-Romero, M Barria, I Olmedo, A Clos, VS Ramanujam, A Urayama, L Vergara, MJ Kogan, C Soto (2010). Bioaccumulation and toxicity of gold nanoparticles after repeated administration in mice. *Biochem Biophys Res Commun* 393:649–655

Luty-Błocho M, K Fitzner, V Hessel, P Löb, M Maskos, D Metzke, K Pacławski, M Wojnicki (2011). Synthesis of gold nanoparticles in an interdigital micromixer using ascorbic acid and sodium borohydride as reducers. *Chem Eng* 171:279–290

Mamiya Y (1983). Pathology of the pine wilt disease caused by *Bursaphelenchus xylophilus*. *Annu Rev Phytopathol* 21:201–220

Markus J, D Wang, YJ Kim, S Ahn, R Mathiyalagan, C Wang, DC Yang (2017). Biosynthesis, characterization, and bioactivities evaluation of silver and gold nanoparticles mediated by the roots of Chinese herbal *Angelica pubescens* Maxim. *Nanoscale Res Lett* 12; Article 46

Mishra A, M Kumari, S Pandey, V Chaudhry, K Gupta, C Nautiyal (2014). Biocatalytic and antimicrobial activities of gold nanoparticles synthesized by *Trichoderma* sp. *Bioresour Technol* 166:235–242

Muniyappan N, N Nagarajan (2014). Green synthesis of gold nanoparticles using *Curcuma pseudomontana* essential oil, its biological activity and cytotoxicity against human ductal breast carcinoma cells T47D. *J Environ Chem Eng* 2:2037–2044

Muthukumar T, B Sambandam, A Aravinthan, TP Sastry, JH Kim (2016). Green synthesis of gold nanoparticles and their enhanced synergistic antitumor activity using HepG2 and MCF7 cells and its antibacterial effects. *Proc Biochem* 51:384–391

Muthuvel A, K Adavallan, K Balamurugan, N Krishnakumar (2014). Biosynthesis of gold nanoparticles using *Solanum nigrum* leaf extract and screening their free radical scavenging and antibacterial properties. *Biomed Prevent Nutr* 4:325–332

Ojea-Jiménez I, NG Bastús, V Puntes (2011). Influence of the sequence of the reagents addition in the citrate-mediated synthesis of gold nanoparticles. *J Phys Chem C* 115:15752–15757

Proença DN, R Francisco, CV Santos, A Lopes, L Fonseca, IM Abrantes, PV Morais (2010). Diversity of bacteria associated with *Bursaphelenchus xylophilus* and other nematodes isolated from *Pinus pinaster* trees with pine wilt disease. *PLoS One* 5; Article e15191

Rai A, A Prabhune, CC Perry (2010). Antibiotic mediated synthesis of gold nanoparticles with potent antimicrobial activity and their application in antimicrobial coatings. *J Mater Chem* 20:6789–6798

Rajan A, V Vilas, D Philip (2015). Catalytic and antioxidant properties of biogenic silver nanoparticles synthesized using *Areca catechu* nut. *J Mol Liq* 207:231–236

Sabry AKH (2019). Role of nanotechnology applications in plant-parasitic nematode control. *In: Nanobiotechnology Applications in Plant Protection*, pp:223–240. Springer, The Netherlands

Sadeghi B, M Mohammadzadeh, B Babakhani (2015). Green synthesis of gold nanoparticles using *Stevia rebaudiana* leaf extracts: Characterization and their stability. *J Photochem Photobiol B Biol* 148:101–106

Servin A, W Elmer, A Mukherjee, RDL Torre-Roche, H Hamdi, JC White, P Bindraban, C Dimkpa (2015). A review of the use of engineered nanomaterials to suppress plant disease and enhance crop yield. *J Nanopart Res* 7; Article 92

Shine DJ, S Shasha, O Emmanuel, SS Fometu, W Guohua (2020). Biosynthesizing gold nanoparticles with *Parkia biglobosa* leaf extract for antibacterial efficacy *in vitro* and photocatalytic degradation activities of rhodamine b dye. *Adv Sci Eng Med* 12:970–981

Shinya R, H Morisaka, Y Takeuchi, K Futai, M Ueda (2013). Making headway in understanding pine wilt disease: What do we perceive in the postgenomic era? *J Biosci Bioeng* 116:1–8

Singleton P (2004). *Bacteria in biology, biotechnology and medicine*, 6th Edition. John Wiley & Sons, Chichester, UK

Spencer RC (2007). Potential bio-terror agents. *J Hosp Infect* 65:19–22

Spencer RC (2003). *Bacillus anthracis*. *J Clin Pathol* 56:182–187

Srivastava N, M Mukhopadhyay (2015). Biosynthesis and characterization of gold nanoparticles using *Zooglea ramigera* and assessment of its antibacterial property. *J Clust Sci* 26:675–692

Su C, Y Ji, S Liu, S Gao, S Cao, X Xu, C Zhou, Y Liu (2020). Fluorescence-labeled abamectin nanopesticide for comprehensive control of pinewood nematode and *Monochamus alternatus* hope. *ACS Sustain Chem Eng* 8:16555–16564

Tenaillon O, D Skurnik, B Picard, Denamur E (2010). The population genetics of commensal *Escherichia coli*. *Nat Rev Microbiol* 8:207–217

Thakur R, P Shirkot (2017). Potential of biogold nanoparticles to control plant pathogenic nematodes. *J Bioanal Biomed* 9:220–222

Tsyusko OV, JM Unrine, D Spurgeon, E Blalock, D Starnes, M Tseng, G Joice, PM Bertsch (2012). Toxicogenomic responses of the model organism *Caenorhabditis elegans* to gold nanoparticles. *Environ Sci Technol* 46:4115–4124

Udobi C, J Onaolapo (2009). Phytochemical analysis and antibacterial evaluation of the leaf stem bark and root of the African locust bean (*Parkia biglobosa*). *J Med Plants Res* 3:338–344

Vallet-Regí M, B González, I Izquierdo-Barba (2019). Nanomaterials as promising alternative in the infection treatment. *Intl J Mol Sci* 20; Article 3806

Vicente CS, F Nascimento, M Espada, M Mota, S Oliveira (2011). Bacteria associated with the pinewood nematode *Bursaphelenchus xylophilus* collected in Portugal. *Antonie van Leeuwen* 100:477–481

Wingfield M, R Blanchette, T Nicholls, K Robbins (1982). Association of pine wood nematode with stressed trees in Minnesota, Iowa, and Wisconsin [*Bursaphelenchus xylophilus, Dothistroma pini, Dioryctria zimmermani, Pinus* spp., insect vectors]. *Plant Dis* 66:934–937

Xu ZC, CM Shen, CW Xiao, TZ Yang, HR Zhang, JQ Li, HL Li, HJ Gao (2007). Wet chemical synthesis of gold nanoparticles using silver seeds: A shape control from nanorods to hollow spherical nanoparticles. *Nanotechnology* 18:1-5

Zhang J, X Li, Y Yang (2014). Screening of disinfectants and their selective toxicity at lower temperature to *Bursaphelenchus xylophilus* and bacteria. *J Chem Pharm Res* 6:2144–2149

Zhao BG, J Tao, YW Ju, PK Wang, JL Ye (2011). The role of wood-inhabiting bacteria in pine wilt disease. *J Nematol* 43:129–134